THE JOURNAL OF BIOLOGICAL CHEMISTRY
Vol. 277, No. 52, Issue of December 27, pp. 50237–50244, 2002
Printed in U.S.A.

Peroxisome Proliferator-activated Receptor α (PPARα) Influences Substrate Utilization for Hepatic Glucose Production*

Received for publication, February 6, 2002, and in revised form, August 6, 2002
Published, JBC Papers in Press, August 9, 2002, DOI 10.1074/jbc.M201208200

Jun Xu‡§¶, Gary Xiao‡§, Chuck Trujillo‡§, Vicky Chang‡§, Lilia Blanco‡§, Sean B. Joseph‖, Sara Bassilian, Mohammed F. Saad§, Peter Tontonoz‖‡‡§§, W. N. Paul Lee**, and Irwin J. Kurland‡§‡‡¶¶**

*From the §Department of Medicine, the ‡Laboratory of Metabolomics, the ¶Department of Biological Chemistry, the ‖Department of Pathology, David Geffen School of Medicine at UCLA, Los Angeles, California 90095, ‡‡Molecular Biology Institute, UCLA, Los Angeles, California 90095, and the **Department of Pediatrics, Harbor-UCLA Medical Center, Torrance, California 90502*

The hypoglycemia seen in the fasting PPARα null mouse is thought to be due to impaired liver fatty acid β-oxidation. The etiology of hypoglycemia in the PPARα null mouse was determined via stable isotope studies. Glucose, lactate, and glycerol flux was assessed in the fasted and fed states in 4-month-old PPARα null mice and in C57BL/6 WT maintained on standard chow using a new protocol for flux assessment in the fasted and fed states. Hepatic glucose production (HGP) and glucose carbon recycling were estimated using [U-$^{13}C_6$]glucose, and HGP, lactate, and glycerol turnover was estimated utilizing either [U-$^{13}C_3$]lactate or [2-^{13}C]glycerol infused subcutaneously via Alza miniosmotic pumps. At the end of a 17-h fast, HGP was higher in the PPARα null mice than in WT by 37% ($p < 0.01$). However, recycling of glucose carbon from lactate back to glucose was lower in the PPARα null than in WT (39% *versus* 51%, $p < 0.02$). The lack of conversion of lactate to glucose was confirmed using an [U-$^{13}C_3$]lactate infusion. In the fasted state, HGP from lactate and lactate production were decreased by 65 and 55%, respectively ($p < 0.05$) in PPARα null mice. In contrast, when [2-^{13}C]glycerol was infused, glycerol production and HGP from glycerol increased by 80 and 250%, respectively ($p < 0.01$), in the fasted state of PPARα null mice. The increased HGP from glycerol was not suppressed in the fed state. While little change was evident for phosphoenolpyruvate carboxykinase (PEPCK) expression, pyruvate kinase expression was decreased 16-fold in fasted PPARα null mice as compared with the wild-type control. The fasted and fed insulin levels were comparable, but blood glucose levels were lower in the PPARα null mice than in controls. In conclusion, PPARα receptor function creates a setpoint for a metabolic network that regulates the rate and route of HGP in the fasted and fed states, in part, by controlling the flux of glycerol and lactate between the triose-phosphate and pyruvate/lactate pools.

The transition through the fasting and refeeding cycle is an important metabolic adaptation in response to food availability and food intake. The adaptation allows the optimization of fuel energy substrate utilization switching from a glucose-and-fatty acid oxidation to a glucose-and-fatty acid storage state. It is believed that these metabolic changes are effected by the reciprocal action of insulin and glucagon. However, the recent availability of animals with specific nuclear receptor disorders, such as the PPARα KO mice, have drawn attention to the linkage between the regulation of fatty acids by the nuclear receptor family and glucose metabolism. PPARα is a member of the nuclear hormone receptors, the peroxisome-proliferator-activated receptors (PPARs),[1] for which fatty acids are ligands (reviewed in Refs. 1, 2). PPARα controls the expression of a number of genes involved in mitochondrial and peroxisomal β-oxidation and plays an important role in maintaining energy homeostasis (reviewed in Refs. 1, 2) during fasting. PPARα KO mice, fasted for 24 h, exhibit severe hypoglycemia, ketonuria, hypothermia, and elevated free fatty acids (FFA) (3, 4). The etiology of the fasting hypoglycemia has not been well characterized. Studies of changes in mRNA expression for the gluconeogenic enzymes phosphoenolpyruvate carboxykinase (PEPCK) and G6Pase p36 catalytic subunit from fast to fed state showed a lack of causal relationship between gluconeogenic enzymes and the observed hypoglycemia (3, 5). *In vivo* studies to establish the relationship between PPARα and insulin action showed that the absence of PPARα did not affect the insulin tolerance test (6) and intraperitoneal glucose tolerance test (3, 6) when wild-type and PPARα null mice were maintained on a chow diet.

The etiology for the hypoglycemia seen in the fasting PPARα null mouse is believed to reflect a depletion of liver glycogen and a decrease in gluconeogenesis secondary to impaired liver fatty acid β-oxidation (3, 4). We report here a study of the regulation of HGP and substrate utilization for PPARα null mice maintained on a chow diet, during the physiologic situation of a moderate overnight fast (17 h) and refeeding (5 h), using ^{13}C-mass isotopomer distribution analysis (MIDA). The measurement of substrate flux utilization is based on the novel use of the Alza miniosmotic pump to supply a continuous infusion of one of three tracers, [U-$^{13}C_6$]glucose, [U-$^{13}C_3$]lactate, or

* This work was supported by a grant from the American Diabetes Association (to I. J. K.) and Grants DK56090-A1 (to W. N. P. L.) and HL66088 (to P. T.). The GC/MS Facility is supported by United States Public Health Service Grant P01-CA42710 to the UCLA Clinical Nutrition Research Unit, Stable Isotope Core and Grant M01-RR00425 to the General Clinical Research Center. The costs of publication of this article were defrayed in part by the payment of page charges. This article must therefore be hereby marked "*advertisement*" in accordance with 18 U.S.C. Section 1734 solely to indicate this fact.

§§ Assistant investigator of the Howard Hughes Medical Institute at the University of California, Los Angeles, CA 90095.

¶¶ To whom correspondence should be addressed. Tel.: 818-634-6953; Fax: 310-825-8534; E-mail address: irwinjk@earthlink.net.

[1] The abbreviations used are: PPAR, peroxisome proliferator-activated receptor; KO, knockout; FFA, free fatty acids; PEPCK, phosphoenolpyruvate carboxykinase; HGP, hepatic glucose production; GC/MS, gas chromatography/mass spectrometry; RT, reverse transcription; MIDA, mass isotopomer distribution analysis; V-A, venous-arterial; A-V, arterial-venous; PEP, phosphoenolpyruvate; triose-P, triose-phosphate; WT, wild type.

TABLE I
TAQMAN Primer and Probe Design

The TAQMAN system is designed to have a fluorescent and quencher tagged probe bind to the region amplified between the forward and reverse primers for the cDNA amplification reaction (after the RT step). The TAQ polymerase hydrolyzes the probe during the extension reaction, releasing the fluorescent tag from the proximity of the quencher, and thereby each amplification cycle can be detected, allowing for the accurate, quantitative determination of the linear region of RT-PCR amplification. The fluorescent tag is attached to the 5′ end of the TAQMAN probe, and the quencher tag (TAMRA) is attached to the 3′ end of the TAQMAN probe. The fluorescent tag FAM was used for pyruvate kinase and PEPCK, and VIC was used for β-actin, allowing for sufficient spectral differentiation so that pyruvate kinase/β-actin or PEPCK/β-actin RT-PCR reactions could be run as multiplex reactions within the same tube.

Target	Primers	TAQMAN Probe
β-actin	FWD: 5′-TCTGTGTGGATTGGTGGCTCTA REV: 5′-CTCCTGCTTGCTGATCCACAT	5′-CCTGGCCTCACTGTCCACCTTCCA-3′
PEPCK	FWD: 5′-TTGCGACAGGCAAGGTCA REV: 5′-CTTGGGCAACTTGGCTGC	5′-CATGCTCAGCCAGTGCGCCAG-3′
Pyruvate kinase	FWD: 5′-CCTCTGCCTTCTGGATATCGAC REV: 5′-CGATGGTGGCAATGATGCT	5′-CAGAGCCTGTGGCCGCTAGGAGC-3′

[2-^{13}C]glycerol. This form of metabolomic profiling uncovers the "silent" phenotype not seen in previous studies of PPARα KO mice and insulin action and indicates that PPARα is an important element regulating metabolic transition from fed to fasted states. The data indicate that the actions of PPARα intersect with those of insulin in the regulation of substrate utilization for hepatic glucose production.

MATERIALS AND METHODS

Animal Studies—The PPARα −/− mice on a C57BL/6 background were a generous gift from Frank J. Gonzalez and have been described (6). The PPARα +/+ mice (C57BL/6) were obtained from colonies maintained by the National Institutes of Health. Animal studies were conducted in accordance with the ILACUC guidelines after approval by our Institutional Review Board. All experiments were performed with male mice ranging from 16 to 18 weeks in age. The average weight of the PPARα +/+ mice was 25.7 ± 1.9 grams, and the average weight of the PPARα −/− mice was 29.9 ± 5 grams. All mice were maintained on standard chow (NIH-31 sterilizable diet 7013, purchased from Harlan Teklad, Madison, WI).

Fasting was initiated at 5 p.m. An Alza miniosmotic pump (model 2001D, Alza, Palo Alto, CA) was inserted between 7 and 8 p.m. The pump contained either 60 mg of [2-^{13}C]glycerol, 50 mg of [U-$^{13}C_3$]lactate, or 50 mg of [U-$^{13}C_6$]glucose, each dissolved in 200 μl of water. The quantity of tracer is sufficient to last through the experiment infusing at a factory-calibrated pump rate of 8 μl per hour. The minipump is inserted in the subcutaneous space, and therefore infusion conditions approximate those of the venous-arterial (V-A) mode of infusion and sampling. Plasma glucose, lactate, and glycerol were sampled in the fasting state between 10 am 11 am. The mice undergoing an [U-$^{13}C_6$]glucose study were sacrificed in the fasting state. The mice undergoing the [2-^{13}C]glycerol and [U-$^{13}C_3$]lactate studies were then refed standard chow (NIH-31 sterilizable diet 7013) and sacrificed between 3 and 4 pm. The animals consumed virtually all of their chow eaten within 2 h of refeeding. At the time of sacrifice, animals were killed by an overdose of isoflurane anesthesia, and tissue from liver and skeletal muscle were rapidly dissected free, snap-frozen in liquid nitrogen, and stored at −80 °C until processed for isolation of RNA or glycogen.

RNA Extraction and Analysis—Total RNA was prepared from ~100 mg of liver after extraction with a guanidinium HCl/phenol mixture (7) following Roche Molecular Biochemicals Tripure Isolation Reagent protocol. Typically, 100 μg of total RNA are obtained from one extraction.

Assessment of Pyruvate Kinase and PEPCK Enzyme mRNA Levels by TAQMAN RT-PCR—The TAQMAN system is designed to have a fluorescent- and quencher-tagged probe bind to the region amplified between the forward and reverse primers for the cDNA amplification reaction (after the RT step). The TAQ polymerase hydrolyzes the probe during the extension reaction, releasing the fluorescent tag from the proximity of the quencher, and thereby each amplification cycle can be detected allowing for the accurate, quantitative determination of the linear region of RT-PCR amplification. Specifically, the number of cycles necessary to reach the threshold for linear amplification of the cDNA (the C_T value) is obtained. The 2^{-C_T} reflects the total mRNA abundance for a given target RNA, the higher the C_T the lower the abundance of the target mRNA. Normalization of the target mRNA to a housekeeping reference is given by $2^{-C_T}/2^{-C_R}$ or $2^{(C_R-C_T)} = 2^{-\Delta C_T}$. When this result is normalized to a baseline, as for example a Me_2SO control for an experiment with insulin-signaling inhibitors dissolved in Me_2SO, the relative abundance of the target mRNA to the housekeeping reference mRNA, normalized to the Me_2SO control, is $2^{-\Delta C_T}$ condition/$2^{-\Delta C_T}$ $Me_2SO = 2^{\Delta\Delta C_T}$. This RT-PCR system affords easy screening with only ~100 ng needed for each measurement, which are done in triplicate for accuracy. In all RT-PCR assessments, measures were taken to avoid amplification of a region of genomic DNA or other contaminants. Target and reference RT-PCR reactions (for example, PEPCK as a target and β-actin for reference) were run singly and then together as a multiplex reaction. The primer concentrations were adjusted in the multiplex reaction tube such that accurate C_T values are obtained, but soon after, the exhaustion of primers defines the end of the reaction. In this way, amplification of the majority species is stopped before it can limit reactants available for amplification of the minority species. Table I shows the primer pairs and labeled probes used in these TAQMAN RT-PCR studies.

Biochemical Analyses—Plasma glucose and lactate concentrations were determined by COBAS MIRA analyzer (Roche Molecular Biochemicals) using reagents provided by Raichem (San Diego, CA). Glucose UV Reagent (Catalog no. 80017) was used for glucose determination, and Stat-Pack Rapid Lactate Test (Catalog no. 869218) was used for lactate. Liver and muscle glycogen were determined after liver or muscle tissues were homogenized and then sonicated in 0.1 N sodium acetate buffer, pH 4.5 (1 ml of buffer/100 mg of tissue). The resulting homogenates were incubated with amylglucosidase (Roche Molecular Biochemicals) overnight at 37 °C. Cellular debris was removed by centrifugation. The supernatant containing glycogen glucose was then desalted using both anion and cation exchange columns (Dowex-1 and Dowex-50, Sigma). The concentration of glucose in the neutral fraction was determined for the calculation of liver or muscle glycogen and for gas chromatography/mass spectrometry (GC/MS) analysis. The amount of liver or muscle glycogen is calculated and reported as μg of glucose/mg of liver or muscle. Stable isotopes (99% enriched) were purchased from ISOTEC (Miamisburg, OH).

Derivatization of Metabolites for GC/MS Analysis—100–150 μl of blood plasma was deproteinized, deionized, and dried. Liver or muscle glycogen glucose extract was also dried. The glucose and glycerol were treated with hydroxylamine hydrochloride and then acetic anhydride to create aldonitrile pentaacetate derivatives for GC/MS analysis according to a modification of the method of Szafranek *et al.* (8). The procedure converts glucose to its aldonitrile pentaacetate derivative and glycerol into its triacetyl ester derivative. The resulting glucose or glycerol derivative was dissolved in 150 μl of ethyl acetate for GC/MS analysis. Lactate was extracted with ethyl acetate and converted to its lactic acid n-propylamide-heptafluorobutyric ester according to the method of Tserng *et al.* (9). The lactate derivative was dissolved in 150 μl of methylene chloride for GC/MS analysis.

GC/MS—All isotopomeric determinations were performed on a Hewlett Packard Mass Selective Detector (model 5973A) connected to a

Hewlett Packard Gas Chromatograph (model 5890) using either chemical ionization (for glucose, glycerol, and lactate derivatives) or electron impact ionization (for glucose derivative only) (8). Glucose and glycerol derivatives were separated on a HP5 capillary column, 30 meters × 250 micrometers internal diameter. GC conditions were helium as carrier gas at a flow rate of 1.0 ml/min; sample injector temperature was 250 °C; and oven temperature was programmed from 220 to 250 °C at a ramp of 10 °C/min. The retention time for the glucose aldonitrile pentaacetate was 2.9 min. Different temperature programming was used for glycerol (from 140 to 230 °C at a ramp of 20 °C/min) and lactate (from 100 to 160 °C at a ramp of 20 °C/min). Retention times were 5.2 min and 3.9 min for the glycerol and lactate, derivatives respectively.

Chemical ionization conditions were with 20% methane. The glucose aldonitrile pentaacetate derivative gives the molecular ion (C1–C6) of the glucose molecule at *m/z* 328. Electron impact ionization of the aldonitrile derivative was used to characterize glucose positional isotopomers at *m/z* 187 for C3–C6 and *m/z* 242 for C1–C4 fragments. The ion clusters monitored for glycerol acetyl ester were from *m/z* 158 to *m/z* 164 with *m/z* 159 corresponding to unlabeled glycerol. Selected ion monitoring was used to follow specific ions. For glucose isotopomer determination, the ion clusters monitored were from *m/z* 327 to *m/z* 336 with a fragment of *m/z* 328 corresponding to unlabeled glucose. The ion clusters monitored for lactate isotopomers were from *m/z* 327 to *m/z* 332 with a fragment of *m/z* 328 corresponding to unlabeled lactate.

Data Calculation and Interpretation—Mass isotopomer distribution is determined using the method of Lee *et al.* that corrects contribution of derivatizing agent and natural ^{13}C abundance to mass isotopomer distribution of the compound of interest (10, 11). The method also corrects for the presence of small amounts of M4 and M5 in the infused [U$^{13}C_6$]glucose. Results of the mass isotopomers in glucose, glycerol, or lactate are reported as molar fractions of m0, m1, m2, etc. according to the number of labeled carbons in the molecule (10, 11). The enrichment of a certain ^{13}C-labeled molecule is defined as its molar fraction m_i, the fraction of molecules with i being the number of ^{13}C substitutions. m_i = labeled molecules with i being the ^{13}C/(total number of molecules). The sum of all isotopomers of the molecules, Σm_i for $i = 0$ to n ($n = 3$ or 6 for lactate/glycerol or glucose, respectively), is equal to 1 or 100%.

Calculation of Production Rates (PR)—Substrate production or turnover rates were determined using the principle of tracer dilution. At isotopic steady state, the production rate of a substrate is given by the following general equation (reviewed in Ref. 12).

$$\text{PR} = (\text{isotope infusion rate}) \times [(\text{infused isotope enrichment})/(\text{final substrate enrichment}) - 1] \quad \text{(Eq. 1)}$$

In the case of glucose production rate, HGP = working pump rate × [(isotope enrichment)/(final substrate enrichment) –1]. The "correction" mentioned under "Materials and Methods" (10, 11) adjusts the impurities in the administered [U-$^{13}C_6$]glucose infused so that the enrichment can be considered to be 100%. M6 = final substrate enrichment.

$$\text{HGP (mg/min/kg)} = \text{working pump rate/M6} - \text{working pump rate} \quad \text{(Eq. 2)}$$

Similarly, glycerol production rate (mg/min/kg) can be calculated as in the following equation.

$$\text{Gly PR} = (\text{working pump rate/m1}) - \text{working pump rate} \quad \text{(Eq. 3)}$$

Lactate production rate can be calculated as in the following equation.

$$\text{lactate PR (mg/min/kg)} = (\text{working pump rate/m3}) - \text{working pump rate} \quad \text{(Eq. 4)}$$

Note that capital M represents molar fraction of glucose; lowercase m represents molar fraction of glycerol or lactate. It should be noted that except for the glucose production rate, the estimation of the lactate and glycerol production rate is dependent on the site of infusion and site of sampling. Since the minipumps were inserted subcutaneously, the experimental conditions approximate those of a V-A mode of infusion and sampling. The lactate and glycerol production rate obtained by such a V-A mode of infusion and sampling is known to be less than the rate obtained by the A-V mode of infusion and sampling (13, 14).

Calculation of Glucose Molecule Recycling—The basis for calculation of glucose molecule recycling has been extensively discussed by Landau *et al.* (15, 16). Theoretically, one molecule of [U-$^{13}C_6$]glucose is converted into two molecules of [U-$^{13}C_3$]lactate/pyruvate through glycolysis. The [U-$^{13}C_3$]lactate can be reutilized for gluconeogenesis such that one molecule of m3 lactate can be recycled as m1, m2, or m3 phosphoenolpyruvate (PEP). We therefore calculated the glucose molecule recycling (FRC) using m1, m2, and m3 isotopomers of lactate and M1, M2, and M3 isotopomers of glucose using the formula of Landau *et al.* (16).

D_L = dilution of labeled lactate by unlabeled lactate

$$= [0.5\ (M_1 + M_2 + M_3) + M_6]/(m_1 + m_2 + m_3) \quad \text{(Eq. 5)}$$

The fractional contribution of glucose to lactate synthesis = $1/D_L$.

F = fraction of the glucose molecules in the blood that recycled

$$= [0.5\ (M_1 + M_2 + M_3)]/[0.5\ (M_1 + M_2 + M_3) + M_6] \quad \text{(Eq. 6)}$$

Combining Equations 5 and 6, the fractional contribution (FRC) of the newly synthesized glucose recycled from lactate is shown in the following equation.

$$\text{FRC (recycled)} = D_L \times F \quad \text{(Eq. 7)}$$

Calculation of Fractional Contribution of Lactate and Glycerol to Gluconeogenesis—The concept of glucose molecule recycling via lactate can be applied to [U-$^{13}C_3$]lactate and [2-^{13}C]glycerol infusion studies. Fractional contribution from lactate (Lactate FRC) is given by the following two equations.

$$\text{Lactate FRC} = [(M1 + M2 + M3)/2(m1 + m2 + m3)] + [(M4 + M5 + M6)/(m1 + m2 + m3)] \quad \text{(Eq. 8)}$$

$$\text{HGP from lactate (mg/min/kg)} = \text{Lactate PR} \times \text{Lactate FRC} \quad \text{(Eq. 9)}$$

Similarly, fractional contribution from glycerol (Glycerol FRC) is given by the following equation.

$$\text{Glycerol FRC} = (M1/2m1) + (M2/m1) \quad \text{(Eq. 10)}$$

$$\text{HGP from glycerol (mg/min/kg)} = \text{glycerol PR} \times \text{glycerol FRC} \quad \text{(Eq. 11)}$$

Since lactate and glycerol production rates may be underestimated by the V-A mode of infusion and sampling, such underestimation may result in similar underestimation of their contribution to gluconeogenesis (14).

Calculation of Fractional Gluconeogenesis by MIDA—When high amounts of [2-^{13}C]glycerol is infused, the condensation of two labeled glycerol molecules (via triose-P) in gluconeogenesis results in three isotopomer species M0, M1, and M2 of glucose. From the distribution of glucose isotopomers, it is possible to deduce precursor (triose-P) enrichment (p) and fraction of new glucose (FSR) using combinatorial algebra (reviewed in Ref. 17).

$$\text{Triose-P enrichment} = p = 2M2/(M1 + 2M2) \quad \text{(Eq. 12)}$$

The fractional contribution of glycerol to the triose-P pool can be calculated when plasma glycerol enrichment (glyE) is determined. It is given by the following expression.

$$p/\text{glyE} = p/\text{m1 of glycerol} \quad \text{(Eq. 13)}$$

The fractional glucose synthesis rate due to gluconeogenesis (FSR) can be determined by

$$\text{FSR} = \text{observed M1/theoretical M1} = M1/[2p(1 - p)] \quad \text{(Eq. 14)}$$

This calculated FSR has been shown to be independent of the mode of infusion and sampling because the recombination occurs at the site of synthesis and is not dependent on the enrichment at the site of sampling (14). The difference between FSR and FRC from lactate or glycerol is that FSR describes how much newly synthesized glucose comes from triose-P pool, while FRC describes how much of this newly synthesized glucose comes from glycerol or lactate. Thus, theoretically, FSR is always greater than FRC.

Statistical Analyses—Analyses for the significance of differences were performed using Student's *t* test, except for analyzing whether steady state isotopomer enrichments occurred in the fasted state (Fig. 1). For the data in Fig. 1, analysis of variance with Tukey's post-test was used.

TABLE II
Biochemical data for WT-C57BL/6 and PPARα KO mice

Mice were fasted for 17 hours and refed standard laboratory chow for 5 hours. Statistical comparisons are between fasted values or fed values only; fed and fasted values are not compared. * and # indicate $p < 0.001$. ** indicates $p < 0.01$. For fasted and fed glycogen levels, the numbers represent an average for all mice used, regardless of tracer. See "Material and Methods" for measurement techniques.

	WT		PPAR KO	
	Fasted	Fed	Fasted	Fed
Glucose (mg/dl)	122 ± 18*	251 ± 30#	73 ± 10*	153 ± 45#
Glucose (mM)	6.78 ± 1*	13.9 ± 1.7#	4.05 ± 0.56*	8.5 ± 2.5#
Insulin (ng/ml)	0.06 ± 0.1	0.88 ± 0.49	0.16 ± 0.19	0.58 ± 0.23
Lactate (mmol/liter)	3.24 ± 0.67	7.03 ± 0.45	3.25 ± 0.50	6.19 ± 1.16
Muscle glycogen (μg/mg)	0.21 ± 0.1	0.26 ± 0.09**	0.07 ± 0.02	0.125 ± 0.07**
Liver glycogen (μg/mg)	3.97 ± 2.29	19.40 ± 8.85#	6.34 ± 2.46	5.71 ± 3.97#

RESULTS

In our paper, the results of lactate turnover and glycerol turnover as well as their contribution to glucose production were calculated based on the V-A mode. Comparison between PPAR knockout and wild-type is based on the same V-A mode. As noted by Beylot and co-workers in their recent paper (14) in the rat, glycerol turnover rate as well as the percent contribution of glycerol to total glucose production is higher in the A-V mode than those obtained from the V-A mode. This trend has also been extensively documented for lactate infusion. However, the ease of surgery (~3 min local procedure for minipump placement) and freedom of unrestricted movement after minipump placement make up for any possible increase in measurement of turnover rates from an A-V method. The A-V method would require more extensive surgery and stress due to excessive blood draws needed for the standard euglycemic-hyperinsulinemic clamp procedure, as well as stress due to restricted movement in a small rodent such as a mouse.

Glucose Homeostasis in the Fasted and Fed States—The WT mice were able to maintain a normal blood glucose concentration of 122 mg/dl after an overnight fast (Table II). The level increased to 251 mg/dl 5 h after feeding. The PPARα KO mice had lower plasma glucose than WT controls in both the fasted and fed states (Table II). There was no significant difference in fasted or fed insulin levels between the PPARα KO mice and the WT controls. The low plasma glucose in the PPARα KO mice was associated with normal lactate levels in the fasted and fed states. Glycogen content in the liver and muscle of the PPARα KO mice was lower than that of the control WT mice in the fed state, but no difference was seen for both strains in the fasted state.

Since the Alza miniosmotic pump has not previously been used for tracer infusion in metabolic studies, we have carried out separate experiments to demonstrate the achievement of isotopic steady state of both the fasted and refed studies. Fig. 1 shows the M6 and M3 enrichment in glucose and m3 enrichment in lactate after an overnight [U-$^{13}C_6$]glucose infusion. Plasma m3 lactate is very constant between 15–19 h of infusion. There is no statistically significant difference in the M6 glucose enrichment or in the conversion of M6 to M3 glucose. Fig. 2 shows the time course of the enrichment of the m1 glucose, m1 lactate, and m1 glycerol in the 17-h fasted and refed states in response to an overnight constant infusion of [2-^{13}C]glycerol by the minipumps. The achievement of metabolic and isotope steady state, between 4 and 5 h after refeeding, is evident.

Table III shows HGP, dilution of blood glucose carbon, and fractional contribution of lactate to glucose as measured by the dilution and recycling of [U-$^{13}C_6$]glucose. The enrichment of M6 glucose in the 17-h fasted state was 30% higher in WT control than in the PPARα KO, and correspondingly the calculated HGP is 37% higher in the PPARα KO than in the WT. The increase in HGP seen for the PPARα KO mouse raises the question whether the increased HGP is secondary to gluconeogenesis, and if so, what are the major gluconeogenic substrates used when PPARα is absent? Examining glucose carbon recycling provides part of the answer. The fasted glycogen levels are the same, statistically, between the PPARα KO and the WT control so tracer dilution differences are not a factor. The breakdown of [U-$^{13}C_6$]glucose results in the formation of m3 triose phosphate/lactate, and the reconversion of m3 triose phosphate/lactate back to glucose leads to labeled glucose with three ^{13}C carbons (M3 glucose). Using the assumption that every labeled lactate molecule recycles as another labeled molecule in glucose (Equation 8), we calculated the recycling of labeled lactate. In the fasted state, 51% of glucose carbons were

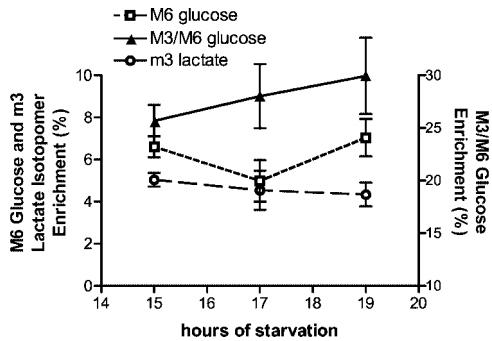

FIG. 1. **Mass isotopomer enrichment in glucose and lactate after an overnight infusion of [U-$^{13}C_6$]glucose administered by Alza miniosmotic pump (see "Materials and Methods") in 4-month-old C57BL/6 (background strain) mice.** Isotopic steady state of glucose and lactate enrichments is attained at 15, 17, and 19 h of infusion during the fast. The variability in isotopomer enrichments seen from the expanded *y*-axis scales used can be expected from the relatively small number of mice used for each point ($n = 3$); however, no statistically significant differences were evident by analysis.

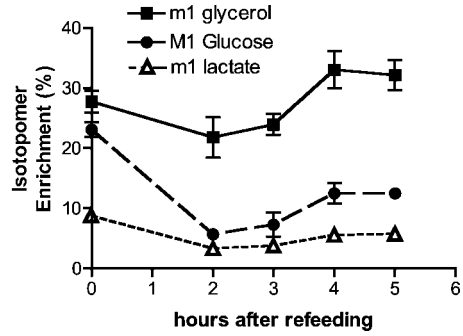

FIG. 2. **Mass isotopomer enrichment in glucose and lactate after an overnight infusion of [2-^{13}C]glycerol administered by Alza miniosmotic pump (see "Materials and Methods") in 4-month-old C57BL/6 (background strain) mice.** $n = 3$ for each time point. Glucose, glycerol, and lactate enrichments after [2-^{13}C]glycerol infusion were measured 17 h into the fast (0 h), and 2, 3, 4, and 5 h after refeeding of a mixed meal. Isotopic steady state is seen between 4 and 5 h after refeeding.

TABLE III
Glucose production and conversion for WT-C57BL/6 and PPARα KO mice

Mice were fasted for 17 hours. * indicates $p < 0.01$, and ** indicates $p < 0.02$. See "Materials and Methods" for formulas used for calculation of substrate production and conversion.

	WT	PPARα KO
Hepatic glucose production (mg/Kg/min) [U-$^{13}C_6$]glucose	8.37 ± 0.6	11.42 ± 1*
Plasma M6 glucose [U-$^{13}C_6$]glucose	11.7 ± 1.23%	9.00 ± 0.65%**
D_L = Dilution of labeled lactate from unlabeled lactate	1.95 ± 0.11	1.52 ± 0.10*
F = fraction of glucose cycled	51.3 ± 5%	39.1 ± 1%**

recycled in the WT, as compared with 39% of glucose carbons in the PPARα KO. The lower recycling in PPARα KO indicates the presence of a partial block in the conversion of lactate to glucose.

The decrease in the muscle glycogen store for the PPARα KO mouse is expected to contribute to a smaller dilution of blood glucose-labeled carbons. This effect is seen in the dilution factor of blood lactate. When a mole of [U-$^{13}C_6$]glucose undergoes glycolysis, 2 moles of m3 lactate is formed. The lactate dilution factor reflects the dilution of labeled lactate by unlabeled lactate, resulting from the metabolism by unlabeled glycogen-glucose to lactate by muscle, for example, in the transition between the fed and fasted states. The reciprocal of blood glucose contribution to lactate is the lactate dilution factor, D_L (see "Materials and Methods"), which is correspondingly decreased in the PPARα KO. Note, that both fed liver and muscle glycogen are lower in the measurements seen for the PPARα KO mice (Table II), in agreement with less dilution seen in the fasted state. In the WT mice, blood glucose contributed about 51% of the lactate in circulation (1/1.95 × 100, see Table III). This contribution was higher in the PPARα KO being 66% (1/1.52 × 100, see Table III). The product of lactate dilution factor, D_L, and the glucose carbon recycling, F, reflects gluconeogenesis from blood lactate. Gluconeogenesis from lactate is almost 100% in the WT in contrast with 59% in the PPARα KO. Gluconeogenesis was further studied using a [2-^{13}C]glycerol infusion. The combination of two labeled triose-P to form glucose with two ^{13}C carbons (M2 glucose) was exploited to determine precursor enrichment and gluconeogenic fraction of the glucose synthesis rate (FSR). The results are shown in Fig. 3. In the fasted state, FSR approached 100% in both WT and PPARα KO. In the fed state, the FSR was suppressed in the WT controls, which could be an effect by insulin, dilution of isotopomer enrichments by unlabeled glucose coming from the gut, or from glycogenolysis in the liver. However, no decrease in the FSR is seen for the PPARα KO mice, resulting in a relative increase of 170% in the FSR in the fed state for the PPARα KO mouse.

Lactate Utilization—The indication of a partial block in lactate utilization was further explored by observing the response to the infusion of [U-$^{13}C_3$]lactate. Infusion of [U-$^{13}C_3$]lactate resulted in higher m3 lactate enrichments in the fasted and fed states for the PPARα KO mouse than the corresponding fasted and fed values in the WT (Table IV). The enrichment of [U-$^{13}C_3$]lactate can be diluted by tissue production of unlabeled lactate or by exchange through its equilibration with pyruvate and alanine. Such dilution through isotope exchange is of theoretical and practical concern, and for this reason, even though our measurements are made at an isotopic steady state, we will refer to lactate production measurements as the "apparent" lactate production. Fig. 4 shows that a 50% decrease in the apparent lactate production in the fasted state and a 75% decrease in the apparent lactate production in the fed state was evident for the PPARα KO mouse *versus* the WT control. There was no significant difference in the lactate levels between the PPARα KO and WT mice in the fasted and fed states (Table II). Thus, lactate utilization and/or isotopic exchange of lactate with alanine, pyruvate, etc., is correspondingly decreased when PPARα is absent.

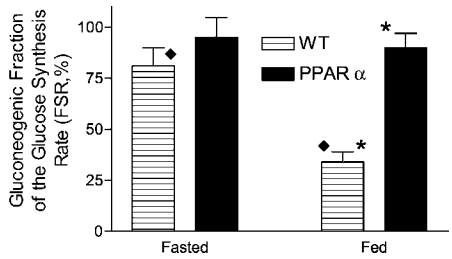

FIG. 3. **Shown is the fractional glucose synthesis rate due to gluconeogenesis (FSR, see Equation 14) measured in the 17-h fasted state and after 5 h of refeeding for the PPARα KO mice and WT C57BL/6 control using a [2-^{13}C]glycerol infusion administered by Alza miniosmotic pump (see "Materials and Methods").** FSR percentages are expressed as the mean ± S.E. from at least four separate experiments. ♦ and * indicate $p < 0.0001$.

Glycerol Utilization—Table IV shows the enrichment of m1 glycerol during the [2-^{13}C]glycerol infusion. Infusion of [2-^{13}C]glycerol resulted in a 40% decrease in the enrichment of m1 glycerol in the fasted state and a 30% decrease in the enrichment of m1 glycerol in the fed state. The difference in enrichment translates into a difference in the calculated rates of glycerol production for the PPARα KO mouse *versus* the control. Fig. 5 shows that glycerol production in the 17-h fasted state was 60–80% higher in the PPARα KO mouse than the wild-type control. The conversion of triose-P to pyruvate/lactate directly, or after its conversion to glucose, results in m1 plasma lactate. The m1 plasma lactate enrichment for the PPARα KO mouse, in response to the [2-^{13}C]glycerol infusion, is equivalent to the fraction of lactate produced from glycerol. This lactate fractional production was 25% less in the fasted state and 15% less in the fed state than the wild-type control (Table IV). Thus, despite the increased glycerol production, conversion of glycerol to lactate is decreased for the fasted state and may also be decreased for the fed state.

Enzymes of Pyruvate Substrate Cycle—The demonstration of a block in the conversion of lactate to glucose and glycerol to lactate could indicate a block in the expression of enzymes in the PEP/pyruvate substrate cycle that are sensitive to the metabolic state. Fig. 6 shows the expression of PEPCK and pyruvate kinase in the fasted state of the PPARα KO mouse *versus* the wild-type control as measured using TAQMAN RT-PCR. While little change is evident for PEPCK expression, pyruvate kinase expression is decreased 16-fold with respect to the wild-type control ($\Delta\Delta C_T \sim 4$). These results suggest that either PEPCK is not a key factor in mediating hepatic PPARα action and/or posttranscriptional mechanisms may affect the amount/regulation of flux between pyruvate and PEP. The decreased pyruvate kinase expression is consistent with the decreased conversion of glycerol to lactate.

Substrates for Glucose Production—In light of the results indicating that PPARα KO is hypoglycemic despite a mildly increased HGP, we examined the rate of glucose synthesis from glycerol and lactate. Results are shown in Figs. 4 and 5. For the PPARα KO mouse, hepatic glucose production from lactate was

TABLE IV
Lactate and glycerol conversion for WT-C57BL/6 and PPARα KO mice

Mice were fasted for 17 hours and refed standard laboratory chow for 5 hours. Statistical comparisons are between fasted values or fed values only; fed and fasted values are not compared. * indicates $p < 0.01$, and ** indicates $p < 0.05$.

	WT		PPARα KO	
	Fasted	Fed	Fasted	Fed
Plasma m3 lactate [U-$^{13}C_3$]lactate	3.62 ± 0.42%**	1.99 ± 0.65%*	6.26 ± 1.31%**	6.19 ± 0.21%*
Plasma m1 glycerol [2-^{13}C]glycerol	33.0 ± 4.0%*	34.0 ± 6%	19.1 ± 3.78%*	22.9 ± 2.1%
Fraction of lactate produced from glycerol [2-^{13}C]glycerol	9.96 ± 1.08%*	7.67 ± 2.1%	7.42 ± 0.89%*	6.51 ± 1.09%

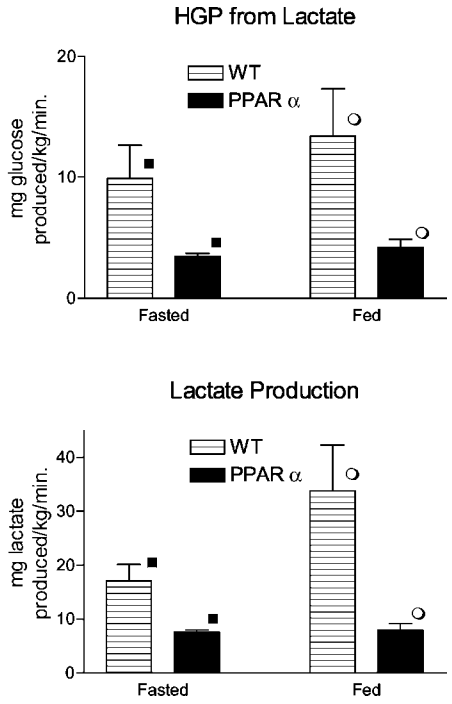

FIG. 4. **HGP from lactate (see "Materials and Methods," Equation 9) (*top panel*) and the lactate production rate (see "Materials and Methods," Equation 4) (*bottom panel*).** Both were measured after 17 h of fasting and 5 h of refeeding for the PPARα KO mice and WT C57BL/6 control using a [U-$^{13}C_3$]lactate infusion administered by Alza miniosmotic pump (see "Materials and Methods"). HGP and lactate production rates are expressed in terms of mg produced/kg of body weight/minute as the mean ± S.E. from at least four separate experiments. ■ and ○ indicate $p < 0.05$.

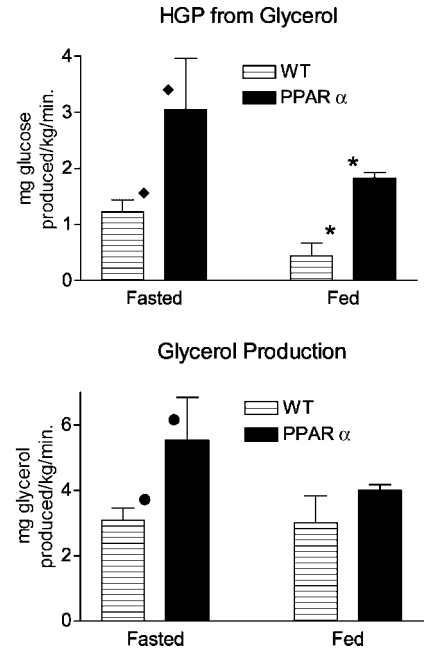

FIG. 5. **HGP from glycerol (see "Materials and Methods," Equation 9) (*top panel*) and the glycerol production rate (see "Materials and Methods," Equation 3) (*bottom panel*).** Both were measured after 17 h of fasting and 5 h of refeeding for the PPARα KO mice and WT C57BL/6 control using a [U-$^{13}C_6$]glucose infusion administered by Alza miniosmotic pump (see "Materials and Methods"). HGP and glycerol production rates are expressed in terms of mg produced/kg of body weight/minute as the mean ± S.E. from at least four separate experiments. * and ♦ indicate $p < 0.01$; ● indicates $p < 0.02$.

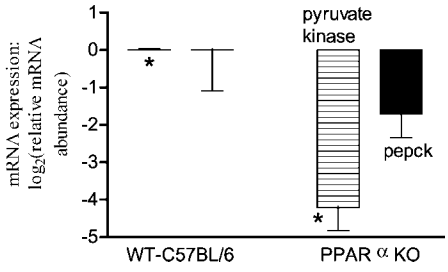

FIG. 6. **The effect of 17 h fast and 5 h refeeding (standard chow) on hepatic PEPCK and pyruvate kinase mRNA expression for the WT and PPARα KO mice.** Total RNA was extracted from liver obtained from mice of both strains and analyzed by quantitative TAQMAN RT-PCR (PerkinElmer Life Sciences). In comparison to the C57BL/6 control, the abundance of PEPCK, or pyruvate kinase relative to that of β-actin is $2^{\Delta\Delta C_T}$. The $\log_2$ (relative mRNA abundance change) is equivalent to the normalized threshold cycle numbers, $\Delta\Delta C_T$ (see "Materials and Methods") and are expressed as the mean ± S.E. from at least four separate experiments.

to be ~3-fold decreased in either the fasted state or fed state as compared with the WT control. Decreases in lactate production mirrored the changes in HGP from lactate. Compensating for the reduced glucose production from lactate, hepatic glucose production from glycerol was to be 2.5-fold increased in the fasted state and 4-fold increased in the fed state for PPARα KO mice as compared with the WT controls. These results further indicate profound changes in glucose, lactate, and glycerol fluxes and their utilization, when PPARα is absent.

DISCUSSION

The PPARα KO mouse is known to have defective fatty acid β-oxidation. It is considered to be an excellent model for the study of disorders of β-oxidation. PPARα KO mice exhibit severe hypoglycemia, hypoketonemia, hypothermia, and elevated FFA when fasted (3, 4). It has long been suspected that the hypoglycemia is secondary to an impairment in hepatic gluconeogenesis due to a lack of obligatory cofactors (ATP, NADH, acetyl-CoA) resulting from decreased fatty acid oxidation (5, 6). We have carried out stable isotope tracer studies to investigate the substrate utilization for hepatic glucose production in PPARα KO mice. In the fasted state, blood glucose in the PPARα KO was maintained by a slightly elevated rate of hepatic glucose production. Glucose carbon recycling was reduced, and gluconeogenic fraction from lactate was only 66% as opposed to 51% for the WT. The observation of reduced gluconeogenesis from lactate is consistent with the 20% reduction

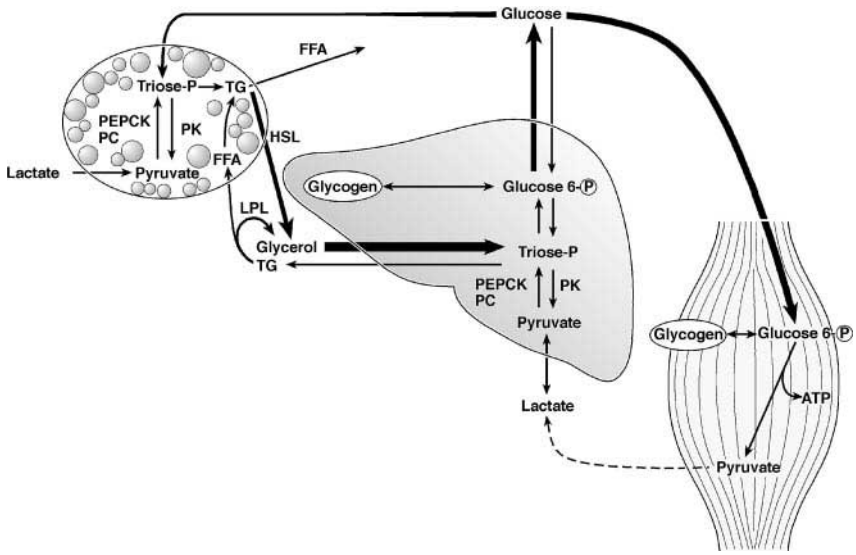

FIG. 7. **The Cori cycle between lactate/pyruvate and glucose serves to transport energy from the liver to peripheral tissues as glucose.** The glucose/glycerol cycle exists primarily between the adipose tissue and the liver. Our data indicate the existence of an interaction between these two futile cycles, dependent on the presence of PPARα. The increased width of the hepatic glycerol flux arrow and the decreased width of muscle lactate flux arrow reflect the changes seen for the PPARα KO mouse glucose metabolome. The PPARα KO mouse has a less active Cori cycle and a more active glucose/glycerol cycle compared with the WT (*LPL*, lipoprotein lipase; *HSL*, hormone-sensitive lipase). Note that the hypoglycemia seen in the fasted and fed states for the PPARα KO mouse, despite increased hepatic glucose production, implies the possibility of increased glucose utilization by muscle.

of gluconeogenesis from lactate/pyruvate in hepatocytes derived from the PPARα KO mouse by Le May *et al.* (5). When gluconeogenesis was estimated using [2-^{13}C]glycerol and MIDA, we found that the gluconeogenic fraction contribution to blood glucose of PPARα KO was comparable to that of the WT control, being nearly 100%, suggesting sources other than lactate as significant gluconeogenic substrates.

Under conditions where the contribution of glycogenolysis to blood glucose is minimal, lactate/pyruvate and gluconeogenic amino acids are the predominant substrates for gluconeogenesis (18). Previous studies suggest that the contribution that glycerol makes plays a minor role (7, 19, 20). Our finding in the WT that HGP from glycerol being about one-tenth of the total HGP is consistent with that view. The plasma glycerol production rate (glycerol R_a) reflects mainly adipose lipolysis (11, 21) because measurements of fatty acid turnover have been found to be consistent with the production of glycerol from the intracellular hydrolysis of triglycerides (reviewed in Ref. 21). In long-term fasting, 15–20% of systemic glycerol turnover may not be due to lipolysis of adipose tissue triglyceride but rather may be due to the hydrolysis of triglyceride circulating as very low density lipoprotein (22). Circulating glycerol is mostly taken up by the liver and utilized for glucose production (15, 19, 20). Thus, conditions that affect lipolysis can have a major influence on the relative contribution of glycerol to gluconeogenesis. In experiments by Jahoor *et al.* (23) inhibition of lipolysis with nicotinic acid resulted in a 16–20% reduction in glucose production and a 50% reduction in glycerol $R_{a.}$ Glucose production was restored by glycerol infusion alone (23). Work by Roden *et al.* (24) indicates that only high FFA concentrations have a stimulatory effect on gluconeogenesis. In the PPARα KO, glycerol production rate after a 17-h fast was 80% higher than that in the WT. The contribution of glycerol to gluconeogenesis when PPARα was absent was correspondingly increased to about 50% as compared with the 10% in the WT. In the PPARα KO, lactate production rate and the glucose production from lactate was greatly reduced. The complementary relationship between lactate production and glycerol production readily suggests the existence of two futile cycles between 3-carbon substrates (glycerol and lactate) and 6-carbon substrate (glucose and glycogen) as depicted in Fig. 7. The cycling between lactate/pyruvate and glucose is the well known Cori cycle, which serves to transport energy from the liver to the peripheral tissues as glucose. In the process, 3-carbon substrates are conserved. On the other hand, the cycling between glycerol and glucose has been less well appreciated. The glycerol cycle also transports energy fuel substrate in the form of triglycerides. However, fatty acid β-oxidation in peripheral tissues and the liver is required. The interaction between these two futile cycles has not been well characterized. In the PPARα KO fasted for 24 h, the reduced β-oxidation was associated with elevation of FFA, which may also reflect increased lipolysis (3). Whether the increased FFA, the reduced β-oxidation, or the elevated glycerol production inhibits lactate production and gluconeogenesis from lactate in the fasted state, or liver glycogen synthesis in the fed state, remains to be investigated.

PPARα KO mice generally do not survive a relatively prolonged fast. This leads to the belief that PPARα is crucial for maintaining energy homeostasis in the adaptive response to fasting (reviewed in Refs. 1, 2). Since insulin is an important hormone that regulates glucose metabolism in the transition from the fasted to fed state, a few studies have been done to examine the role of PPARα in modulating insulin sensitivity and resistance (6, 25, 26). Results of such studies are conflicting. While PPARα activators have been shown to improve insulin sensitivity, (25) under the conditions of high fat feeding the absence of PPARα seems to negate the development of high-fat diet-induced insulin resistance (6, 26). Our data indicate that for the PPARα KO mouse under the physiologic conditions of refeeding, HGP is increased and glycogen synthesis is decreased for the same insulin levels, suggesting a situation of hepatic insulin resistance. Our results are consistent with the finding that PPARα activators improve insulin sensitivity by Guerre-Millo *et al.* (25). However, our observation is opposite to the conclusion of Tordjman *et al.* (26) in their studies of PPARα KO mice with a ApoE KO mouse background. Our study of metabolic adaptation to the fast and fed cycle revealed for the first time that the absence of PPARα affects substrate utilization regardless of the level of insulin. Abnormalities of glucose metabolism, particularly reduced lactate production and glycogen synthesis, are more pronounced in the fed than in the fasted state. The lack of glucose carbon recycling via the Cori cycle and the depletion of liver glycogen in the liver when PPARα is absent promotes a maladaptation to prolonged fast.

In summary, our investigation into hypoglycemia in the PPARα KO mice points to the importance of studying the dynamics of substrate fluxes of both the fed and fasted states. Metabolic abnormalities resulting from specific gene defects may lead to specific abnormalities in substrate fluxes, which limit the adaptation in the transition from fasted to fed states. In the PPARα KO mice, the metabolic abnormality is probably

initiated by the reduced lactate production and conversion to glucose, leading to poor glycogen deposits in both the liver and in the muscles. In the fasted state, PPARα KO mice cannot switch to fatty acid oxidation, which leads to reduced glucose carbon recycling and continued depletion of 6-carbon substrates. Standard characterization of phenotypes using the insulin tolerance test and the intraperitoneal glucose tolerance test showed a silent phenotype for the action of PPARα (3, 26) and failed to reveal any difference for the action of PPARα on insulin action when chow fed. The PPARα KO mouse is a complex glucose metabolic phenotype that can better be understood in the context of glucose metabolome studies (characterization of substrate fluxes within a glucose metabolic network) than the paradigm of insulin sensitivity and insulin resistance, as in traditional studies.

Acknowledgments—We thank Dr. Alan R. Collins, Dept. of Medicine, UCLA, for technical assistance. We are grateful to Dr. Frank Gonzalez (NCI, National Institutes of Health) and Dr. Ron Evans (Salk Institute) for the gift of the PPARα KO mice.

REFERENCES

1. Kersten, S., Desvergne, B., and Wahli, W. (2000) *Nature* **405,** 421–424
2. Desvergne, B., and Wahli, W. (1999). *Endocr. Rev.* **20,** 649–688
3. Kersten, S., Seydoux, J., Peters, J. M., Gonzalez, F. J., Desvergne, B., and Wahli, W. (1999) *J. Clin. Invest.* **103,** 1489–1498
4. Leone, T. C., Weinheimer, C. J., and Kelly, D. P. (1999). *Proc. Natl. Acad. Sci. U. S. A.* **96,** 7473–7478
5. Le May, C., Pineau, T., Bigot, K., Kohl, C., Girard, J., and Pegorier, J. P. (2000) *FEBS Lett.* **475,** 163–166
6. Guerre-Millo, M., Rouault, C., Poulain, P., Andre, J., Poitout, V., Peters, J. M., Gonzalez, F. J., Fruchart, J. C., Reach, G., and Staels, B. (2001) *Diabetes* **50,** 2809–2814
7. Chomczynsky, P., and Sacchi, N. (1987) *Anal. Biochem.* **162,** 156–159
8. Szafranek, J., Pfaffenberger, D. C., and Horning, E. C. (1974) *Carbohydr. Res.* **38,** 97–105
9. Tserng, K. Y., Gilfillan, C. A., and Kalhan, S. C. (1984) *Anal. Chem.* **56,** 517–523
10. Lee, W. N. P. (1989) *J. Biol. Chem.* **264,** 13002–13004
11. Lee, W. N. P., Edmond, J., Byerley, L. O., and Bergner, E. A. (1990) *Biol. Mass. Spectrom.* **20,** 451–458
12. Wolfe, R. R. (1992) in *Radioactive and Stable Isotope Tracers in Biomedicine*, pp. 119–144, John Wiley & Sons, Inc., New York
13. Katz, J., and Wolfe, R. R. (1988) *Metabolism* **37,** 1078–1080
14. Peroni, O., Large, V., Odeon, M., Beylot, M. (1996) *Metabolism* **45,** 897–901
15. Landau, B. R. (1999) *Am. J. Physiol.* **277,** E408–E413
16. Landau, B. R., Wahren, J., Ekberg, K., Previs, S. F., Yang, D., Brunengraber, H. (1998) *Am. J. Physiol.* **274,** E954–E961
17. Hellerstein, M. K., and Neese, R. A. (1999) *Am. J. Physiol.* **276,** E1146–E1170
18. Exton, J. H., and Park, C. R. (1967) *J. Biol. Chem.* **242,** 2622–2636
19. Landau, B. R., Wahren, J., Chandramouli, V., Schumann, W. C., Ekberg, K., and Kalhan, S. C. (1996) *J. Clin. Invest.* **98,** 378–385
20. Landau, B. R., Wahren, J., Previs, S. F., Ekberg, K., Chandramouli, V., and Brunengraber, H. (1996) *Am. J. Physiol.* **271,** E1110–E1117
21. Landau, B. R. (1999) *Proc. Nutr. Soc.* **58,** 973–978
22. Jensen, M. D., Chandramouli, V., Schumann, W. C., Ekberg, K., Previs, S. F., Gupta, S., and Landau, B. R. (2001) *Am. J. Physiol. Endocrinol. Metab.* **281,** E998–E1004
23. Jahoor, F., Klein, S., and Wolfe, R. (1992) *Am. J. Physiol.* **262,** E353–E358
24. Roden, M., Stingl, H., Chandramouli, V., Schumann, W. C., Hofer, A., Landau, B. R., Nowotny, P., Waldhausl, W., and Shulman, G. I. (2000) *Diabetes* **49,** 701–707
25. Guerre-Millo, M., Gervois, P., Raspe, E., Madsen, L., Poulain, P., Derudas, B., Herbert, J. M., Winegar, D. A., Willson, T. M., Fruchart, J. C., Berge, R. K., and Staels, B. (2000) *J. Biol. Chem.* **275,** 16638–16642
26. Tordjman, K., Bernal-Mizrachi, C., Zemany, L., Weng, S., Feng, C., Zhang, F., Leone, T. C., Coleman, T., Kelly, D. P., Semenkovich, C. F. (2001) *J. Clin. Invest.* **107,** 1025–1034